Journal of Power Sources 232 (2013) 240–245

Contents lists available at SciVerse ScienceDirect

Journal of Power Sources

journal homepage: www.elsevier.com/locate/jpowsour

Short communication

$Li(Mn_{1/3}Ni_{1/3}Fe_{1/3})O_2$–Polyaniline hybrids as cathode active material with ultra-fast charge–discharge capability for lithium batteries

K. Karthikeyan [a], S. Amaresh [a], V. Aravindan [a,b], W.S. Kim [c], K.W. Nam [d], X.Q. Yang [d], Y.S. Lee [a,*]

[a] Faculty of Applied Chemical Engineering, Chonnam National University, Gwang-ju 500-757, Republic of Korea
[b] Energy Research Institute @ NTU (ERI@N), Nanyang Technological University, Research Techno Plaza, 50 Nanyang Drive, Singapore 637553, Singapore
[c] Daejung EM Co. Ltd., Incheon 405-820, Republic of Korea
[d] Chemistry Department, Brookhaven National Laboratory, Upton, NY 11973, USA

HIGHLIGHTS

- Ultra-fast charge–discharge capability is achieved for Fe based layered composites with polyaniline.
- $Li(Mn_{1/3}Ni_{1/3}Fe_{1/3})O_2$–polyaniline composite delivered reversible capacity of ~110 mAh g^{-1} at 40 C rate.
- Extraordinary performance is mainly due to drastic improvement of electronic conductivity.

GRAPHICAL ABSTRACT

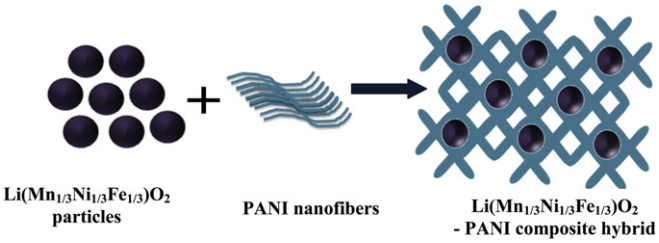

ARTICLE INFO

Article history:
Received 12 November 2012
Received in revised form
10 December 2012
Accepted 12 December 2012
Available online 12 January 2013

Keywords:
Lithium batteries
Polyaniline
Layered material
Cobalt free cathode
High rate

ABSTRACT

We first report the ultra-fast charge–discharge capability of organic–inorganic ($Li(Mn_{1/3}Ni_{1/3}Fe_{1/3})O_2$–Polyaniline (PANI)) nanocomposites prepared by mixed hydroxide route and followed by polymerization of aniline monomers with different concentrations (0.1 and 0.2 mol concentration of PANI). Li-insertion properties are evaluated in half-cell configuration, test cell ($Li/Li(Mn_{1/3}Ni_{1/3}Fe_{1/3})O_2$–PANI) comprising 0.2 mol. PANI delivered the reversible capacity of ~127, ~114 and ~110 mAh g^{-1} at ultra-high current rate of 5, 30 and 40 C, respectively with exceptional cycleability between 2 and 4.5 V *vs.* Li. Such an exceptional performance is mainly due to the conducting pathways promoted by PANI network and it is revealed by impedance measurements. This result certainly provides the possibility of using such layered type Fe based cathode materials in high power Li-ion batteries to drive zero emission vehicles such as hybrid electric vehicles or electric vehicles applications in near future.

1. Introduction

Of late immense research focus is directed toward the development of high capacity, high voltage, low cost and eco-friendly cathode for Li-ion batteries (LIB) typically containing layered structure [1–6]. Since the commercialization of LIBs by Sony Inc. in 1991, layered type $LiCoO_2$ and graphite were dominated as cathode and anode materials, respectively [7]. In such combination, graphitic anode essentially serves as buffer medium during Li-insertion/extraction; hence any advancement in LIB technology relies on the development of high performance cathodes [8–10]. Although the theoretical capacity of Li_xCoO_2 is 274 mAh g^{-1}, complete removal of 1 mol lithium is found difficult due to the structural transformation from hexagonal to cubic which results in severe fade during cycling. Hence, the practical capacity is restricted to ~140 mAh g^{-1}. Apart from the capacity, $LiCoO_2$ displayed

* Corresponding author. Tel.: +82 62 530 1904; fax: +82 62 530 1909.
E-mail addresses: aravind_van@yahoo.com (V. Aravindan), leeys@chonnam.ac.kr (Y.S. Lee).

0378-7753/$ – see front matter
http://dx.doi.org/10.1016/j.jpowsour.2012.12.114

poor high current performance, toxicity of cobalt and its expensiveness is another important concern, therefore search for alternate high performance cathodes is warranted. In this line, other layered type cathodes such as $LiMnO_2$, $LiNiO_2$, $LiFeO_2$ and Li_2MnO_3 were proposed, however practical application of such candidates are too limited due to their own setbacks [10–12]. Eco-friendly, spinel $LiMn_2O_4$ and olivine $LiFePO_4$ were also proposed as potential alternatives, nevertheless former one suffers Mn^{3+} dissolution issue and later compound lacks of conductivity and limited operating potential problems, respectively [13]. Latter, Yabuuchi and Ohzuku [14] reported the performance of layered $LiCo_{1/3}Ni_{1/3}Mn_{1/3}O_2$ cathode with reversible capacity over 200 mAh g^{-1} which is higher capacity than reported elsewhere on layered compounds. On the other hand, aforementioned cathode still contains Co and also suffers high rate operations, which is one of the pre-requisite to power zero emission vehicles such as hybrid electric vehicles (HEV) and electric vehicles (EV). Recently, a series of "cobalt-free" Fe based layered type cathodes were reported by Tabuchi et al. [15,16] and delivered the reversible capacity over 200 mAh g^{-1} in the initial cycles. However, severe capacity fading is encountered for said layered type compounds and also complex synthetic process was employed to yield single phase material and inherent electronic conductivity issues as well. Very recently, we reported Fe based layered type $Li_{1.2}(Mn_{0.32}Ni_{0.32}Fe_{0.16})O_2$ cathodes by a simple sol–gel technique in the presence of adipic acid with good electrochemical properties [17]. As expected, in general Fe based materials are generally experiencing poor electrochemical behavior at high current operations due to the intrinsic nature such compounds [18]. In this line, we made an attempt to synthesize $LiFe_{1/3}Ni_{1/3}Mn_{1/3}O_2$ cathodes by simple co-precipitation technique and followed by annealing. To alleviate the inherent properties of said compound, the concept of making composite cathode was developed by using a conducting polymer, polyaniline (PANI) to form composite inorganic-organic hybrids [19,20]. Among the conducting polymers reported, PANI has certain advantageous likely, higher chemical stability, high electrical conductivity in its oxidized/protonated form, better acid–base properties and stable electrochemical behavior [19]. In addition, few reports based on PANI based composites cathodes were already reported to promote the conducting nature of cathodes, for example $LiFePO_4$–PANI [20–22] and $LiNi_{0.8}Co_{0.2}O_2$–PANI [23]. In the present work, a novel organic–inorganic hybrid $LiFe_{1/3}Ni_{1/3}Mn_{1/3}O_2$–PANI cathode was prepared first time by co-precipitation and followed by sonication with two different concentration of polymer (0.1 and 0.2 mol). Li-insertion properties were evaluated in half-cell configuration with ultra-high rate of 40 C (mass loading of active material 10 mg cm^{-2}) and described in detail.

2. Experimental

The $Li(Mn_{1/3}Ni_{1/3}Fe_{1/3})O_2$ was prepared using a mixed hydroxide method. Analytical grade LiOH (95%), $Fe(NO_3)_3\cdot 9H_2O$ (98%), and $Ni(NO_3)_3\cdot 6H_2O$ (97%) were procured from Junsei chemicals, Japan and $MnCl_2\cdot 4H_2O$ (99.9%) was obtained from Wako Japan and used as such. In the typical synthesis procedure, stoichiometric amounts of transition metal salts were dissolved in distilled water separately and mixed together to enable solution phase reaction. Later, aqueous solution containing LiOH was added by drop wise into the solution and stirred for 6 h to produce mixed hydroxide precipitates. Then the precipitate was aged overnight, filtered and washed to remove residual Li salts and dried at 60 °C for 10 h. The resultant product was obtained by firing the precipitate with slightly excess amount of LiOH at 800 °C for 10 h under oxygen flow.

PANI was synthesized by chemical polymerization method, for instance 0.1 and 0.2 mol of aniline and ammonium persulfate (APS) were separately dissolved in 5 ml of 1 M HCl. Chemical polymerization was initiated by the slower addition of APS into aniline solution. The polymerization was completed within 10 min with formation of highly viscous black precipitate containing PANI. Then hybrid nanocomposites were prepared by the inclusion of 0.1 g of $Li(Mn_{1/3}Ni_{1/3}Fe_{1/3})O_2$ particles into the above solution and sonicated. After 10 min, the black precipitate was filtered, washed several times with deionized water and dried overnight in a vacuum at 60 °C before conducting characterization studies. From the TGA curves (Figure S1), concentration of PANI was ~9.5% (0.1 mol) and ~18.25% (0.2 mol) for $Li(Mn_{1/3}Ni_{1/3}Fe_{1/3})O_2$–P1 and $Li(Mn_{1/3}Ni_{1/3}Fe_{1/3})O_2$–P2 hybrids, respectively.

X-ray diffraction patterns (XRD) were recorded by Rint 1000, Rigaku, Japan using Cu K_α radiation. Surface morphology of the powders was analyzed by transmission electron microscopy (TEM, JEM-2000 FX-II, JEOL, Japan). FT-IR spectroscopic measurements were carried out on IR Prestige-21, Japan spectrometer. The Brunauer–Emmett–Teller (BET) surface area analysis was performed through a Micromeritics ASAP 2010 surface analyzer (Micromeritics, USA). Thermogravimetric analysis (TGA) was performed at 5 °C min^{-1} under oxygen flow using thermal analyzer system (STA 1640, Stanton Redcroft Inc., UK) to estimate the wt.% of PANI. All the electrochemical studies were conducted in two electrode CR 2032 coin-cell configurations. The composite cathodes were prepared by pressing the mixture of 75% active material (10 mg), 15% Ketjen black (2 mg) and 10% Teflonized acetylene black (1.25 mg), TAB-2 in to a 200 mm^2 area stainless steel mesh, which serves as current collector. Before conducting the cell assembly under Ar filled glove box, composite electrode was dried at 160 °C for 4 h in a vacuum oven. The test cells were fabricated with composite cathode and lithium metal as anode which was separated by a porous polypropylene separator (Celgard 3401). 1 M $LiPF_6$-ethylene carbonate/dimethyl carbonate (1:1 vol.) was used as electrolyte solution obtained from Techno Semichem Co., Ltd., Korea. Galvanostatic cycling studies were conducted between 2 and 4.5 V *vs.* Li at different current densities in ambient temperature conditions.

3. Results and discussion

Fig. 1a represents the powder-XRD patterns of pristine $Li(Mn_{1/3}Ni_{1/3}Fe_{1/3})O_2$, $Li(Mn_{1/3}Ni_{1/3}Fe_{1/3})O_2$–PANI-0.1 mol (hereafter abbreviated as $Li(Mn_{1/3}Ni_{1/3}Fe_{1/3})O_2$–P1) and $Li(Mn_{1/3}Ni_{1/3}Fe_{1/3})O_2$–PANI-0.2 mol (hereafter abbreviated as $Li(Mn_{1/3}Ni_{1/3}Fe_{1/3})O_2$–P2). The observed XRD reflections are indexed according to the α-$NaFeO_2$ structure with $R\bar{3}m$ space group. Apparent to notice the formation of phase pure layered structure without any impurity traces, more importantly the absence secondary peaks associated with PANI, which indicates the amount of PANI used to make hybrids are very less and it is too lower for the detectable limitation of XRD instrument. Lattice parameter values are calculated and found to be $a = 2.898$ and $b = 14.311$ Å ($c/a = 4.94$) which is good agreement with similar layered type compound $Li(Mn_{1/3}Ni_{1/3}Co_{1/3})O_2$ by Yabuuchi and Ohzuku [14]. The $I_{(0\,0\,3)}/I_{(1\,0\,4)}$ ratio is found to 1.09 which clearly demonstrate the positive-electrode material contains a good layered structure with very small amount of cation mixing [24,25]. In general, oxygen sub-lattice in the α-$NaFeO_2$ type structure is distorted from the *fcc* array in the direction of hexagonal *c*-axis. This distortion gives rise to splitting of the XRD reflections corresponding Miller indices (0 0 6)/(1 0 2) and (1 0 8)/(1 1 0) which is the characteristic of typical layered structure. Further, there is no deviation from the crystalline peaks noted during sonication with different concentrations of PANI and this suggests the presence of PANI does not affect the structural properties of layered $Li(Mn_{1/3}Ni_{1/3}Fe_{1/3})O_2$. FT-IR spectra were recorded to ensure the

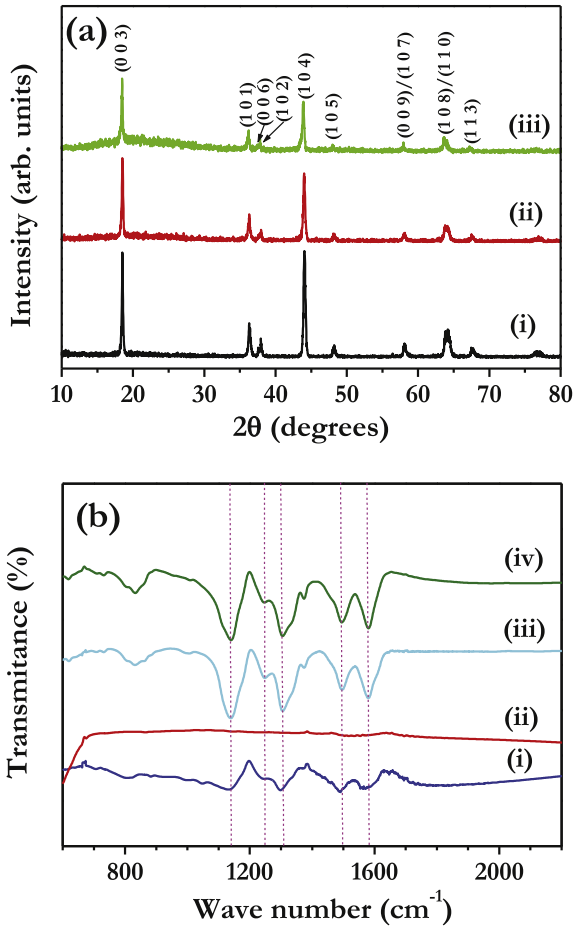

Fig. 1. (a) X-ray diffraction patterns of (i) $Li(Mn_{1/3}Ni_{1/3}Fe_{1/3})O_2$, (ii) $Li(Mn_{1/3}Ni_{1/3}Fe_{1/3})O_2$—P1 and (iii) $Li(Mn_{1/3}Ni_{1/3}Fe_{1/3})O_2$—P2 composite hybrids, and (b) FT-IR spectrum of (i) bulk PANI, (ii) $Li(Mn_{1/3}Ni_{1/3}Fe_{1/3})O_2$, (iii) $Li(Mn_{1/3}Ni_{1/3}Fe_{1/3})O_2$—P1 and (iv) $Li(Mn_{1/3}Ni_{1/3}Fe_{1/3})O_2$—P2.

presence of PANI in the composite and given in Fig. 1b. In PANI, the bands ~1485 and ~1559 cm^{-1} are assigned to benzoid and quinoid ring vibrations, respectively. In case of hybrid composites, vibrational band associated with quinoid rings is slightly shifted toward higher frequencies (~1584 cm^{-1}), whereas there is no much deviation in the benzoid ring vibration is noted. This shifting of vibrational modes clearly reveals that quinoid rings predominate in $Li(Mn_{1/3}Ni_{1/3}Fe_{1/3})O_2$—PANI hybrid composites, and suggests degree of oxidation of polymer is due to their interaction with metal oxide surfaces [26]. In addition, intensity ratio of benzoid and quinoid rings bands is almost unity and confirming the oxidation state of emeraldine salt of PANI [26]. The bands appeared at ~1245 and ~1310 cm^{-1} in hybrid composites corresponding to the stretching vibration of Ph—N and C—NH^+ group of PANI, respectively [27]. Further a strong vibrational peak ~1140 cm^{-1} is the characteristic signature of PANI, which is considered to be a measure of the degree of delocalization of electrons [26,27]. The FT-IR analysis well supported the presence of PANI and its surface interaction with layered compound $Li(Mn_{1/3}Ni_{1/3}Fe_{1/3})O_2$. Electronically conducting nature of PANI and it surface interaction with metal oxide will certainly improves the conducting properties of $Li(Mn_{1/3}Ni_{1/3}Fe_{1/3})O_2$ thereby good electrochemical properties are expected for the said composite.

Morphological features of the prepared phases were investigated through transmission electron microscopy (TEM) and presented in Fig. 2. It is evident to notice that the distribution of $Li(Mn_{1/3}Ni_{1/3}Fe_{1/3})O_2$ particles ranging from 100 to 200 nm in size (Fig. 2a). The layered $Li(Mn_{1/3}Ni_{1/3}Fe_{1/3})O_2$ particles are attached/embedded with PANI and apparently seen from the TEM images (Fig. 2b and c) as clusters. The distribution of $Li(Mn_{1/3}Ni_{1/3}Fe_{1/3})O_2$ particles in the PANI matrix is found uniform for $Li(Mn_{1/3}Ni_{1/3}Fe_{1/3})O_2$—P2 compared to $Li(Mn_{1/3}Ni_{1/3}Fe_{1/3})O_2$—P1. BET surface area is measured and found 5.89, 39.53 and 57.86 $m^2\ g^{-1}$ for $Li(Mn_{1/3}Ni_{1/3}Fe_{1/3})O_2$, $Li(Mn_{1/3}Ni_{1/3}Fe_{1/3})O_2$—P1 and $Li(Mn_{1/3}Ni_{1/3}Fe_{1/3})O_2$—P2, respectively (Figure S2). It is obvious to notice that, higher specific surface is evident for composite hybrids, which increases higher electrode/electrolyte interface and thereby anticipating facile diffusion of Li-ions under high current operations.

Galvanostatic charge—discharge studies were performed in half-cell configuration between 2 and 4.5 V *vs.* Li, at 0.5 C and given in Fig. 3. Typical charge—discharge traces are given in Fig. 3a and test cells delivered the reversible capacities of ~181 and ~138 mAh g^{-1} for $Li(Mn_{1/3}Ni_{1/3}Fe_{1/3})O_2$—P1 and $Li(Mn_{1/3}Ni_{1/3}Fe_{1/3})O_2$—P2, respectively. Apparently, extended monotonous charge—discharge curves for both composites are noted compared to its native form. This is mainly because of the enhanced electronic conductivity offered by the conducting polymer PANI, which also directly promotes the redox reaction of transition metals [18,23]. Higher specific surface area cannot be ruled out for such exceptional performance. On the other hand, pristine $Li(Mn_{1/3}Ni_{1/3}Fe_{1/3})O_2$ displayed the reversible capacity of only ~30 mAh g^{-1} under the same testing conditions. Furthermore, the hybrid composites showed excellent cycleability at low current rate when compared to pristine material (Fig. 3b). The hybrid cathodes revealed good battery characteristics and retained 86 and 80% of capacity after 40 cycles for $Li(Mn_{1/3}Ni_{1/3}Fe_{1/3})O_2$—P2 and $Li(Mn_{1/3}Ni_{1/3}Fe_{1/3})O_2$—P1, respectively with coulombic efficiency over 99.5%. Generally, it is believed that, Fe based compounds are experiencing inherent conductivity issues and hence strong conductive coating/painting is necessary to realize the full capacity [18].

In the case of $Li(Mn_{1/3}Ni_{1/3}Fe_{1/3})O_2$—P1 hybrid, PANI concentration is not sufficient to attain desired level of conductivity enhancement. Further, observed capacity is mainly attributed to the $Mn^{3+/4+}$ and $Ni^{3+/4+}$ redox couples, since utilization of $Fe^{3+/4+}$ redox couple is found difficult in tested potential window for such layered matrix [16]. Hence, transition metal Fe^{3+} essentially act as the matrix element to provide the necessary structural stability during Li-insertion/extraction. Apart from the effective utilization is $Mn^{3+/4+}$ and $Ni^{3+/4+}$ redox couples, usage appropriate amount of PANI is crucial to yield high performance $Li(Mn_{1/3}Ni_{1/3}Fe_{1/3})O_2$—PANI hybrid composites [19,21–23,28]. To realize the role of PANI in layered matrix under high current operations, rate capability studies were conducted for hybrid composites and presented in Fig. 3c. The half-cell Li/$Li(Mn_{1/3}Ni_{1/3}Fe_{1/3})O_2$—P2 delivered a reversible capacities of 181, 163, 158, 148, 132, 120, 114 and 110 mAh g^{-1} at 0.5, 1, 1.5, 3, 5, 15, 30 and 40 C rates respectively, whereas discharge capacities of 136, 133, 126, 113, 95, 87, 73 and 47 mAh g^{-1} are noted for $Li(Mn_{1/3}Ni_{1/3}Fe_{1/3})O_2$—P1 composite hybrids under the same current rate. It is evident that the discharge capacity is decreased at high currents due to the polarization of electrodes and it is mainly due to the less participation of active material. The observed capacity values are much better than the values reported for its parent compound $LiNi_yMn_yCo_{1-2y}O_2$ ($y = 0.5, 0.45, 0.4, 0.33$) by Whittingham and co-workers [29]. Irrespective of the compositions of transition metal ions, maximum deliverable capacity is up to ~30 mAh g^{-1} at current rate of 0.5 C with severe capacity fading. Further in the present case, capacity fading is found very small for $Li(Mn_{1/3}Ni_{1/3}Fe_{1/3})O_2$—P2 hybrid cathodes compared to $Li(Mn_{1/3}Ni_{1/3}Fe_{1/3})O_2$—P1. It is quite interesting to note that, under such harsh conditions (beyond 15 C rate), the $Li(Mn_{1/3}Ni_{1/3}Fe_{1/3})O_2$—P2 composite hybrid showed exceptional reversible capacity values (>100 mAh g^{-1}). Hence, a duplicate cell has been made to

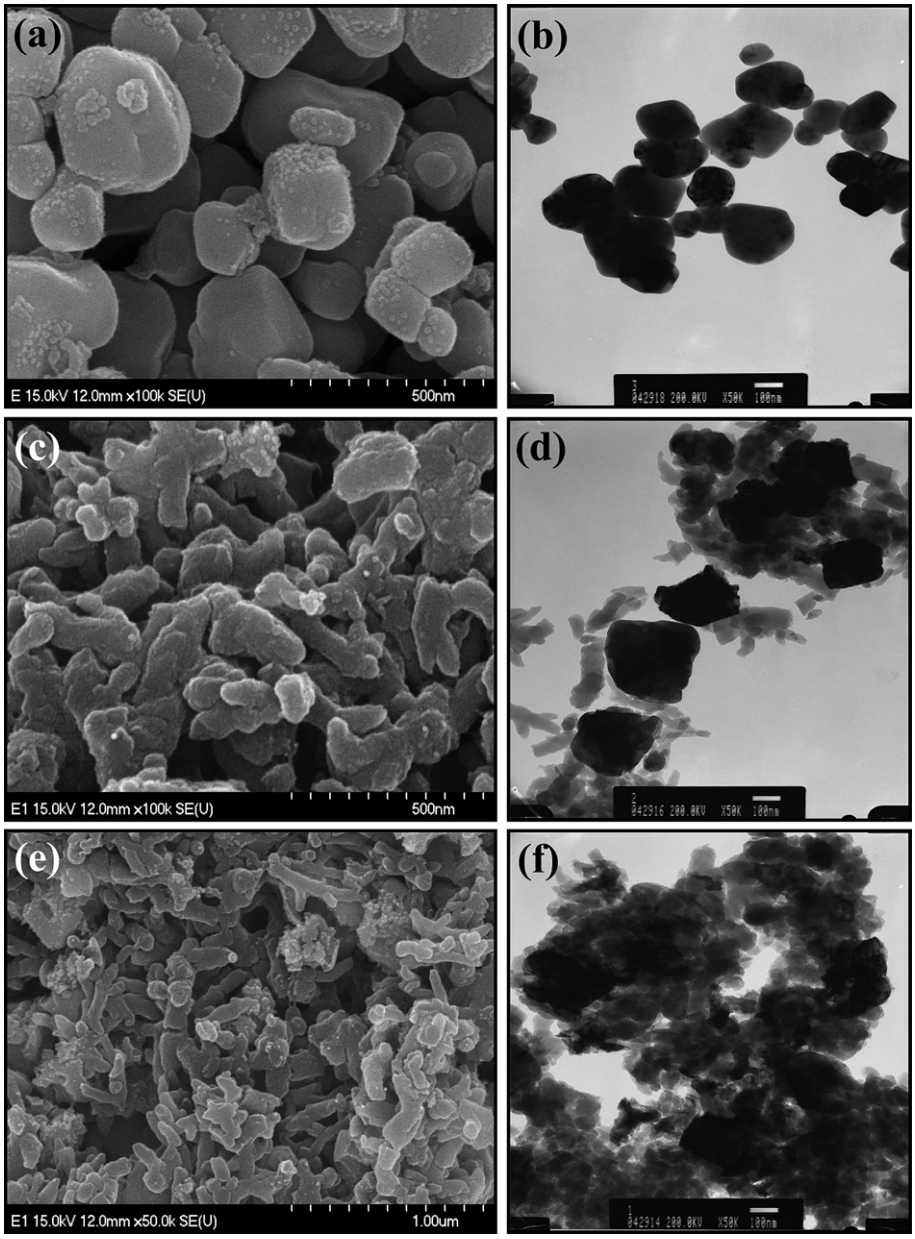

Fig. 2. SEM images of (a) $Li(Mn_{1/3}Ni_{1/3}Fe_{1/3})O_2$ nanoparticles prepared using mixed hydroxide method, (c) $Li(Mn_{1/3}Ni_{1/3}Fe_{1/3})O_2$–P1 and (e) $Li(Mn_{1/3}Ni_{1/3}Fe_{1/3})O_2$–P2 composite materials and TEM images of (b) $Li(Mn_{1/3}Ni_{1/3}Fe_{1/3})O_2$ (d) $Li(Mn_{1/3}Ni_{1/3}Fe_{1/3})O_2$–P1 and (f) $Li(Mn_{1/3}Ni_{1/3}Fe_{1/3})O_2$–P2 hybrid materials.

evaluate the durability of $Li(Mn_{1/3}Ni_{1/3}Fe_{1/3})O_2$–P2 cathode under high current rates and presented in Fig. 4 with active mass loading of 10 mg cm^{-2}. Test cell delivered the discharge capacity of 127, 114 and 110 mAh g^{-1} at 5, 30 and 40 C rates, respectively. However, the difference between reversible capacity at low (5 C) and high (40 C) current rate is noted only 17 mAh g^{-1}. Further, cell retained the discharge capacity of 90% after 100 cycles and this is the outstanding performance among the hybrid cathodes reported [19,21–23]. On the other hand, Li/$Li(Mn_{1/3}Ni_{1/3}Fe_{1/3})O_2$–P1 delivers only about ~90 mAh g^{-1} at 5 C rate (Figure S3) with good cycleability. As the observation from BET, TEM and SEM analysis, relatively large surface area of $Li(Mn_{1/3}Ni_{1/3}Fe_{1/3})O_2$–P2 composite hybrid, more uniformly distributed $Li(Mn_{1/3}Ni_{1/3}Fe_{1/3})O_2$ particles into the porous PANI networks with smaller size, and inherent higher electronic conductivity facilitate the electrons and lithium ions diffusion during intercalation and de-intercalation process, which resulted in the excellent reversibility at high-current rates. The obtained results certainly provide the possibility of using eco-friendly layered $Li(Mn_{1/3}Ni_{1/3}Fe_{1/3})O_2$–PANI composite cathodes in high power applications like HEV and EV. We believe that such an exceptional performance of Fe based cathodes is mainly due to the synthesis of composites with PANI which not only improves the electronic conductivity, but also facilitates electrolyte adsorption through the open polymer matrix and stabilizes the electrode–electrolyte interface, which results the improvement in reversible capacity and rate capability as well [30,31].

To study the influence of polymer matrix toward improvement in the conductivity profiles, an electrochemical impedance spectroscopy (EIS) studies were studied and given in Fig. 3. It is apparent to notice the presence of three main regions, high-frequency semicircle is attributed to the formation of solid electrolyte interface film and/or contact resistance, medium frequency region is

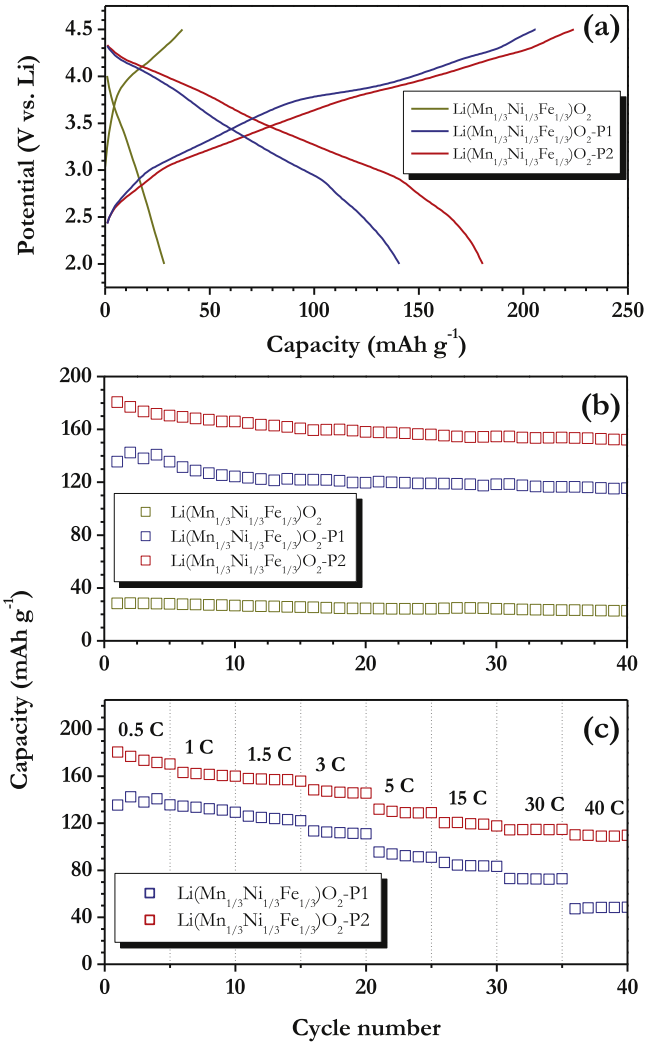

Fig. 3. (a) Typical galvanostatic charge–discharge curves of Li/Li($Mn_{1/3}Ni_{1/3}Fe_{1/3}$)O_2 (or) Li/Li($Mn_{1/3}Ni_{1/3}Fe_{1/3}$)O_2–P1 (or) Li/Li($Mn_{1/3}Ni_{1/3}Fe_{1/3}$)O_2–P2 cells cycled between 2 and 4.5 V at 0.5 C (b) Plot of discharge capacity *vs.* cycle number of above half-cells in ambient temperature conditions and (c) rate performance of studies composite hybrid cathodes with two different concentration of PANI at different C rates.

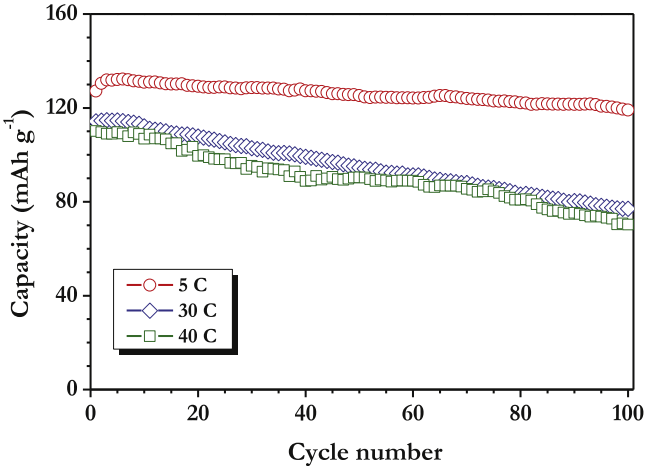

Fig. 4. Reversible capacity *vs.* cycle number of Li($Mn_{1/3}Ni_{1/3}Fe_{1/3}$)O_2–P2 cathodes in half-cell configuration at the C rates of 5, 30 and 40 C.

associated with charge-transfer (R_{ct}) impedance across the electrode/electrolyte interface, and the inclined line at approximately 45° angle to the real axis, which indicates the lithium diffusion kinetics toward the electrodes called as Warburg tail. The direct measurement of R_{ct} corresponds to the electronic conductivity profiles of the materials tested. In this line, the R_{ct} values of the composites hybrids are found 43.4 Ω, 37.5 Ω, 28.1 Ω for Li($Mn_{1/3}Ni_{1/3}Fe_{1/3}$)O_2, Li($Mn_{1/3}Ni_{1/3}Fe_{1/3}$)O_2–P1 and Li($Mn_{1/3}Ni_{1/3}Fe_{1/3}$)O_2–P2, respectively (Fig. 5a). This clearly indicates the enhancement of conductivity profile in the layered Li($Mn_{1/3}Ni_{1/3}Fe_{1/3}$)O_2 matrix after the incorporation of PANI compared to native phase. However, a small amount of PANI concentration is not sufficient (Li($Mn_{1/3}Ni_{1/3}Fe_{1/3}$)O_2–P1) to improve the conductivity for desired level. Higher concentration of PANI in Li($Mn_{1/3}Ni_{1/3}Fe_{1/3}$)O_2–P2 composite delivered good electrochemical profiles which are due to the enhanced electronic conductivity profiles offered by the polymer matrix. Extraordinary performance of Li($Mn_{1/3}Ni_{1/3}Fe_{1/3}$)O_2–P2 at high current rates, EIS traces were recorded after 100 cycles (5 C) Li($Mn_{1/3}Ni_{1/3}Fe_{1/3}$)O_2–P1 and Li($Mn_{1/3}Ni_{1/3}Fe_{1/3}$)O_2–P2 and given in Fig. 5b. Nyquist plot of the Li($Mn_{1/3}Ni_{1/3}Fe_{1/3}$)O_2–P2 cell exhibited a smaller semi-circle compared to Li($Mn_{1/3}Ni_{1/3}Fe_{1/3}$)O_2–P1, which indicates former electrode has a lower R_{ct} values. This lower R_{ct} values (64.59 Ω for Li($Mn_{1/3}Ni_{1/3}Fe_{1/3}$)O_2–P1 and 30.79 Ω for Li($Mn_{1/3}Ni_{1/3}Fe_{1/3}$)O_2–P2) are mainly ascribed to the improvement in electronic conducting profiles supported by the polymer PANI and good adherence properties of the polymer as well. Further, the improved lithium storage properties of the cell containing Li($Mn_{1/3}Ni_{1/3}Fe_{1/3}$)O_2–P2 electrode could be attributed to the polarity of PANI, which is more compatible with the electrolyte, mediating the polarity difference between the active materials and electrolyte. Hence, the electrolyte penetration was promoted to the electro active materials compared with conventional conductive additives like amorphous carbon, carbon nanotube etc. Slightly higher density of PANI compared to carbonaceous materials prevents severe detrimental effects of volumetric capacity. Moreover,

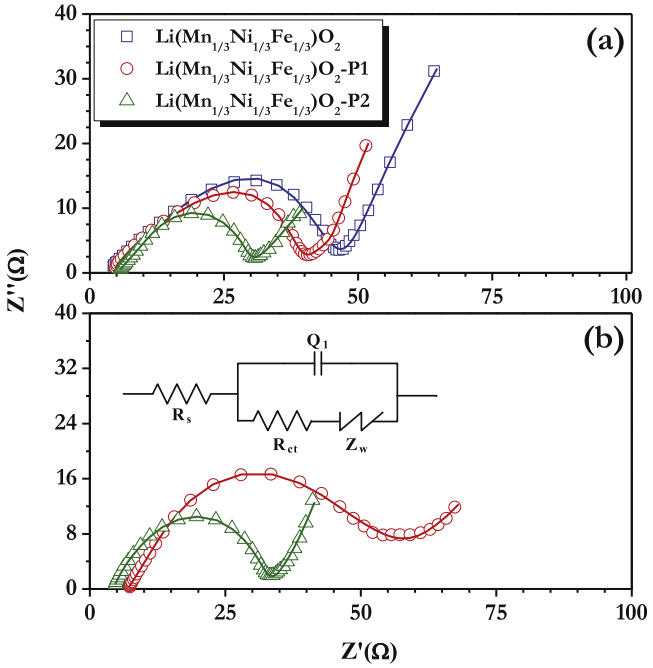

Fig. 5. (a) Nyquist plots of Li/Li($Mn_{1/3}Ni_{1/3}Fe_{1/3}$)O_2, Li/Li($Mn_{1/3}Ni_{1/3}Fe_{1/3}$)O_2–P1 and Li/Li($Mn_{1/3}Ni_{1/3}Fe_{1/3}$)O_2–P2 freshly made cells recorded at open circuit voltage between 100 kHz and 100 mHz, and (b) Nyquist plots of composite hybrids cells measured after 100 cycles. Inset showed equivalent circuit model used for fitting. The line represents the fitted data, and symbol represents the experimental data.

PANI conducting network between the metal oxide particles in $Li(Mn_{1/3}Ni_{1/3}Fe_{1/3})O_2$–P2 composite ensured the electrolyte is more accessible, thereby reducing R_{ct} value and thus enhanced the electrochemical performance of the $Li(Mn_{1/3}Ni_{1/3}Fe_{1/3})O_2$–P2 even at high current rates. The obtained EIS spectra were fitted according to the equivalent circuit model given in the inset. Furthermore, the Nyquist plots of the $Li(Mn_{1/3}Ni_{1/3}Fe_{1/3})O_2$–P2 cell recorded before and after cycled at 5 C for 100 cycles presented in Figure S4. It is evident that, very small variation in the R_{ct} values before and after cycling suggests the less reactivity toward electrolyte counterparts which ensures the enhanced cycleability of $Li(Mn_{1/3}Ni_{1/3}Fe_{1/3})O_2$–P2 under harsh conditions.

4. Conclusion

A novel eco-friendly organic–inorganic hybrid composite with excellent electrochemical performance was demonstrated in half-cell configuration under harsh conditions. The TEM pictures revealed the formation of sub-micron size $Li(Mn_{1/3}Ni_{1/3}Fe_{1/3})O_2$ particles and composite formation with two different concentration of PANI. Among them, $Li(Mn_{1/3}Ni_{1/3}Fe_{1/3})O_2$–PANI (0.2 mol) was exhibiting better battery characteristics and retained 86% of initial discharge capacity after 40 cycles. The composite hybrid, $Li(Mn_{1/3}Ni_{1/3}Fe_{1/3})O_2$ with 0.2 mol. PANI exhibited exceptional cycleability at high current rates (5, 30 and 40 C) with good capacity retention properties. The presence of PANI certainly enhances inherent conducting nature of Fe based compounds and enables facile insertion extraction of Li-ions under such harsh conditions. Demonstration of such high current performance after the incorporation of organic counterpart paved the new way for development of high performance Li-ion batteries and possibly to power the zero emission vehicles in near future.

Acknowledgement

This work was supported by the IT R&D program of MKE/KEIT [KI002176, Development of 3.6 Ah Class Cylindrical Type Lithium Secondary Battery].

Appendix A. Supplementary data

Supplementary data related to this article can be found at http://dx.doi.org/10.1016/j.jpowsour.2012.12.114.

References

[1] V. Aravindan, J. Gnanaraj, Y.S. Lee, S. Madhavi, Journal of Materials Chemistry A (2013). http://dx.doi.org/10.1039/C2TA01393B.
[2] N.-S. Choi, Z. Chen, S.A. Freunberger, X. Ji, Y.-K. Sun, K. Amine, G. Yushin, L.F. Nazar, J. Cho, P.G. Bruce, Angewandte Chemie International Edition 51 (2012) 9994–10024.
[3] A. Manthiram, The Journal of Physical Chemistry Letters 2 (2011) 176–184.
[4] M.S. Whittingham, Proceedings of the IEEE 100 (2012) 1518–1534.
[5] J. Goodenough, Journal of Solid State Electrochemistry 16 (2012) 2019–2029.
[6] C.M. Hayner, X. Zhao, H.H. Kung, Annual Review of Chemical and Biomolecular Engineering 3 (2012) 445–471.
[7] Y. Nishi, The Chemical Record 1 (2001) 406–413.
[8] J.B. Goodenough, Journal of Power Sources 174 (2007) 996–1000.
[9] J.B. Goodenough, Y. Kim, Chemistry of Materials 22 (2009) 587–603.
[10] M.S. Whittingham, Chemical Reviews 104 (2004) 4271–4302.
[11] P. Kalyani, N. Kalaiselvi, Science and Technology of Advanced Materials 6 (2005) 689–703.
[12] J.G. Li, J.J. Li, J. Luo, L. Wang, X.M. He, International Journal of Electrochemical Science 6 (2011) 1550–1561.
[13] O.K. Park, Y. Cho, S. Lee, H.-C. Yoo, H.-K. Song, J. Cho, Energy & Environmental Science 4 (2011) 1621–1633.
[14] N. Yabuuchi, T. Ohzuku, Journal of Power Sources 119–121 (2003) 171–174.
[15] M. Tabuchi, A. Nakashima, H. Shigemura, K. Ado, H. Kobayashi, H. Sakaebe, H. Kageyama, T. Nakamura, M. Kohzaki, A. Hirano, R. Kanno, Journal of The Electrochemical Society 149 (2002) A509–A524.
[16] M. Tabuchi, Y. Nabeshima, T. Takeuchi, H. Kageyama, K. Tatsumi, J. Akimoto, H. Shibuya, J. Imaizumi, Journal of Power Sources 196 (2011) 3611–3622.
[17] K. Karthikeyan, S. Amaresh, G.W. Lee, V. Aravindan, H. Kim, K.S. Kang, W.S. Kim, Y.S. Lee, Electrochimica Acta 68 (2012) 246–253.
[18] S. Okada, J.-i. Yamaki, Journal of Industrial and Engineering Chemistry 10 (2004) 1104–1113.
[19] P. Novák, K. Müller, K.S.V. Santhanam, O. Haas, Chemical Reviews 97 (1997) 207–282.
[20] K.S. Park, S.B. Schougaard, J.B. Goodenough, Advanced Materials 19 (2007) 848–851.
[21] W.-M. Chen, Y.-H. Huang, L.-X. Yuan, Journal of Electroanalytical Chemistry 660 (2011) 108–113.
[22] Y.-H. Huang, J.B. Goodenough, Chemistry of Materials 20 (2008) 7237–7241.
[23] E. Perez-Cappe, Y. Mosqueda, R. Martinez, C.R. Milian, O. Sanchez, J.A. Varela, A. Hortencia, E. Souza, P. Aranda, E. Ruiz-Hitzky, Journal of Materials Chemistry 18 (2008) 3965–3971.
[24] D.-C. Li, T. Muta, L.-Q. Zhang, M. Yoshio, H. Noguchi, Journal of Power Sources 132 (2004) 150–155.
[25] T. Ohzuku, K. Nakura, T. Aoki, Electrochimica Acta 45 (1999) 151–160.
[26] W.-S. Huang, B.D. Humphrey, A.G. MacDiarmid, Journal of the Chemical Society, Faraday Transactions 1: Physical Chemistry in Condensed Phases 82 (1986) 2385–2400.
[27] K.G. Neoh, E.T. Kang, K.L. Tan, Journal of Polymer Science Part B: Polymer Physics 31 (1993) 395–401.
[28] F. Leroux, G. Goward, W.P. Power, L.F. Nazar, Journal of The Electrochemical Society 144 (1997) 3886–3895.
[29] Z. Li, N.A. Chernova, M. Roppolo, S. Upreti, C. Petersburg, F.M. Alamgir, M.S. Whittingham, Journal of The Electrochemical Society 158 (2011) A516–A522.
[30] D. Trivedi, Handbook of Organic Conductive Molecules and Polymers, Conductive Polymers: Synthesis and Electrical Properties, Wiley, 1997.
[31] W.-M. Chen, L. Qie, L.-X. Yuan, S.-A. Xia, X.-L. Hu, W.-X. Zhang, Y.-H. Huang, Electrochimica Acta 56 (2011) 2689–2695.